Optically-Pumped Single-Mode Deep-Ultraviolet Microdisk Lasers With AlGaN-Based Multiple Quantum Wells on Si Substrate

Yiyun Zhang
Hongjian Li
Panpan Li
Arash Dehzangi, *Member, IEEE*
Liancheng Wang, *Member, IEEE*
Xiaoyan Yi
Guohong Wang

Optically-Pumped Single-Mode Deep-Ultraviolet Microdisk Lasers With AlGaN-Based Multiple Quantum Wells on Si Substrate

Yiyun Zhang,[1] **Hongjian Li,**[2] **Panpan Li,**[3]
Arash Dehzangi,[1] *Member, IEEE*, **Liancheng Wang,**[3,5] *Member, IEEE*,
Xiaoyan Yi,[3,4] **and Guohong Wang**[3,4]

[1]Department of Electrical Engineering and Computer Science, Northwestern University, Evanston, IL 60208 USA
[2]Materials Department, University of California, Santa Barbara, CA 93106, United States
[3]Semiconductor Lighting Technology Research and Development Center, Institute of Semiconductors, Chinese Academy of Sciences, Beijing 10083, China
[4]University of Chinese Academy of Sciences, Beijing 100049, China
[5]State Key Laboratory of High Performance Complex Manufacturing, College of Mechanical and Electrical Engineering, Central South University, Changsha 410083, China

Abstract: In this work, we report demonstration of optically-pumped single-mode deep-ultraviolet lasing actions operating at room temperature from $\sim$1-μm 150-nm-thick undercut microdisks with AlN/Al$_{0.35}$Ga$_{0.65}$N (5.5 nm/2.5 nm) multiple quantum wells. These AlGaN-based microdisks are grown on Si substrate by metal-organic chemical vapor deposition. The lasing wavelength centers at $\sim$300.1 nm with the linewidth of $\sim$1.0 nm as the excitation exceeds the lasing threshold of $\sim$24.2 mJ/cm^2. An emission coupling factor (β) of 9.2 $\times$ 10^{-2} is estimated based on the light output characteristics of the AlN/AlGaN microdisks with increasing the pumping densities. Concurrently, a 100 meV blue-shift in the mode energy has also been observed. The lasing spectral peak is attributed to fundamental-order transverse-electric whispering-gallery modes, confirmed by three-dimensional finite-difference time-domain simulations.

Index Terms: Microdisk cavities, deep ultraviolet lasing, whispering-gallery modes.

1. Introduction

Semiconductor solid-state ultra-violet (UV) light sources are ideal candidates to replace traditional mercury UV-lamps, riding on the numerous advantages such as environment friendliness, high-efficiency, longer lifetime and compact structures [1]. Amongst, AlGaN-based UV light-emitters have gained considerable attention owing to their extensive range of applications, including disinfection, water purification, biomedical function, high-density data storage and non-line-of-sight communication [2], [3]. Recently, by means of nano/micro optical cavities, like nanowires [4], [5],

photonic crystals [6], [7], and nanopillars [8], high-quality low-threshold lasing has become achievable with emitting wavelengths reaching the UV range. Meanwhile, GaN microdisk cavities as important alternatives have drawn much interest and emerged as a distinct subject owing to their wide wavelength coverage, high optical gain, small mode volume as well as simple architectures [9]–[12]. As an emerging promising yet competitive technical route, plenty of lasing actions via whispering-gallery modes (WGMs) established in GaN-on-Si microdisks have been demonstrated, covering the span of lasing wavelengths from green [13], blue [14], to near ultraviolet [15]–[17] via adopting different gain mediums, such as InGaN multiple quantum wells (MQWs), bulk GaN, and GaN quantum dots (QDs). Recently, the lasing wavelength has been extended to UVC (275 nm) by using binary GaN/AlN QWs as the optical gain mediums from 3-μm microdisk cavities on Si platform [18], [19]. To increase the band-gap of GaN to the range in which the light emission is pushed into the deep UV range, it is essential for GaN quantum wells to be precisely engineered atomically thin, so that strong quantum confinement can take place [20]. However, this precise engineering method puts great limitations on the growth conditions and facilities, which normally entails using precise but time-consuming growth by molecular beam epitaxy (MBE) system, as it has been implemented by several groups [18], [19], [21]. Therefore, direct use of AlGaN-based QWs grown by metal-organic chemical vapor deposition (MOCVD) as the gain mediums to achieve deep-UV lasing are urgently demanded, with various advantages such as large-area epitaxy, as well as flexibility, fast growth and low cost [22]–[26]. On the other hand, since the emission coupling factor ($\beta \sim 10^{-4}$) has been mainly limited by the multi-mode lasing characteristic of the investigated microdisks, smaller microdisks with reduced mode volume would be more appropriate for high-β micro-lasers [18].

In this study, we report the demonstration of optically-pumped single-mode operated deep UV lasing from AlGaN-based undercut microdisks on Si substrate at room temperature, using AlN/Al$_{0.35}$Ga$_{0.65}$N (5.5 nm/2.5 nm) MQWs grown by MOCVD as the gain mediums. The size of the microdisks has been successfully reduced to 1-μm by adopting microsphere lithography (MSL) technique, which facilitates the reduction in modal numbers existing within the microdisk cavities and thereafter the emission coupling efficiency is achieved close to $\sim$0.1. We also conduct three-dimensional finite-difference time-domain (3D-FDTD) simulation over the related wavelength band to identify the modal family of the lasing peak.

2. Experimental

The microdisk cavities are fabricated using an AlN/AlGaN-based wafer on a two-inch (111) silicon substrate grown by MOCVD (Aixtron). The epitaxy structure consists of a 20 nm-thick low-temperature grown AlN nucleation layer, 80-nm high-temperature grown AlN buffer at 1250 °C, 5 periods of Al$_{0.35}$Ga$_{0.65}$N/AlN (2.5 nm/5.5 nm) MQWs, and a 15 nm AlN cap layer grown at 1000 °C, with a total thickness of around 150 nm. The AlGaN wells and the AlN barriers were grown at 1000 °C and 1110 °C, respectively. To start the fabrication procedure, SiO$_2$ microspheres with average diameters of 1 μm are initially dispersed in de-ionized (DI) water at a low volume ratio of 1:1000. The SiO$_2$ microspheres used here are originally packaged as 2.5% solids (w/v) aqueous suspensions. This low volume ratio ensures that the SiO$_2$ microspheres are properly dispersed and not packed together. It also facilitates the optical pumping to a single microdisk in the PL measurement. After the growth, AlN/AlGaN-Si wafer is treated with simple cleaning and degreasing, and then a droplet of the suspension is then pipetted onto a AlN/AlGaN-Si wafer. Afterwards, the wafer is placed on the hot plate and dried at a temperature of 50 °C to form isolated SiO$_2$ microspheres as the hard masks in the following inductively coupled plasma (ICP, AST Cirie-200) dry-etching process. The ICP system permits to use Chlorine or Fluorine based plasma etching, which in our case, a combination of BCl$_3$ and Ar is selected to perform this important step. To attain smoother sidewalls and proper etching rate, all involved parameters, such as ratios between BCl$_3$ and Ar, flow rates, powers and table temperature were carefully optimized. The AlN/AlGaN-Si wafer is then loaded in the ICP chamber (chiller, 10 °C) and over-etched for 2 min using Ar/BCl$_3$ gases (10 sccm/30 sccm) to create 1 μm AlN/AlGaN-Si micro-pillars. The etch recipe are 500 W
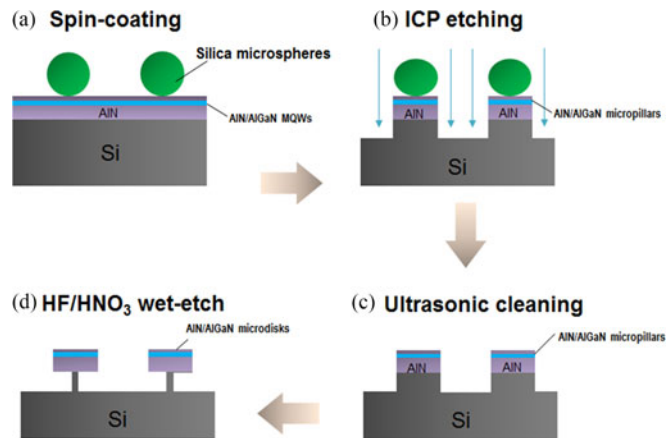
Fig. 1. (a) Schematic diagrams illustrating fabrication process flow for AlGaN/AlN microdisks on Si: (a) spin-coating of Silica micro-beads (b) ICP dry etch for formation of AlGaN/AlN micropillars (c) ultrasonic cleaning to remove residual micro-beads and (d) HF/HNO$_3$ wet etch for 30 s to create undercuts.
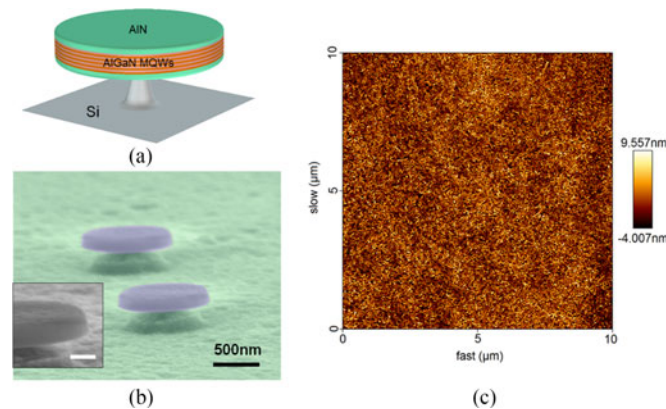

Fig. 2. (a) Schematic diagram of AlGaN/AlN microdisk epi-structure, (b) tilted SEM image of 1-μm undercut AlGaN/AlN microdisks on Si substrate and (c) Atomic force microscopic image showing the surface morphology of the AlN/AlGaN-on-Si wafer. Inset shows the magnified view on the sidewall of AlGaN/AlN microdisk on Si. The scale bar presents a length of 200 nm.

of coil power and 100 W of platen power under a chamber pressure of 5 mTorr. Residual SiO$_2$ microspheres on top of the AlN/AlGaN micropillars are then removed by ultrasonic bath in DI water for 10 min. The wafer is then immersed into a 1:1 HF (10%)/HNO$_3$ (40%) solution for 30 s which partially etches off the beneath Si base, leaving tiny Si posts to mechanically uphold the AlN/AlGaN microdisks. The process flow of fabricating the undercut microdisk cavities can be found in the Fig. 1. Similar processing techniques can be referred in the previous studies as well [14].

3. Results and Discussion

A schematic diagram illustrating the epi-structure for undercut AlN/AlGaN-Si microdisks is shown in Fig. 2(a). The field-emission scanning electronic microscope (FE-SEM) image in Fig. 2(b) shows the 1-μm undercut AlN/AlGaN-based microdisks supported on Si from a tilted angle of 75 degree. Inset shows a zoom-in SEM image showing the very smooth sidewalls of the fabricated microdisk cavities, which plays a critical role in achieving excellent optical confinement for whispering-gallery modes (WGMs) with lower light-scattering loss at the disk edge [9]. To obtain smoother sidewalls, we start the processing by selecting very smooth AlN/AlGaN-Si wafers as the start materials.
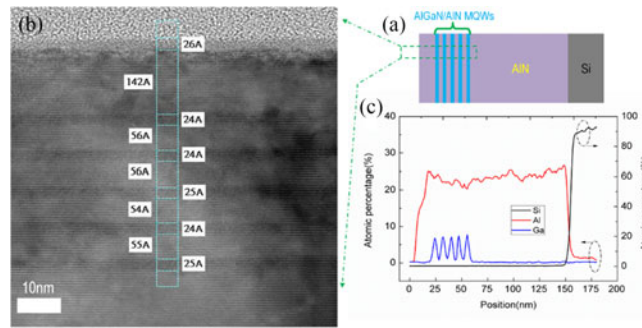
Fig. 3. (a) Schematic diagram of the cross-section of an AlN microdisk with AlGaN MQWs, (b) a TEM image of the AlGaN MQWs, and (c) A linear scanning EDX analysis used for composition distribution across the microdisk cavities.

Meanwhile, a recipe with less Cl_2 gas is adopted in the ICP dry-etching process so as to reduce the masks erosion [27]. Fig. 2(c) presents a typical atomic force microscopic (AFM) image showing the surface morphology of the AlGaN/AlN-on-Si wafer. In fact, we have investigated the surface roughness all over the as-grown AlN/AlGaN-Si wafers by probing an area of $10 \times 10 \ \mu m^2$ at three different regions, and it turns out that the as-grown wafers are crack-free, with smooth and uniform surface. The root mean square (R_q) and arithmetic average (R_a) of height deviation taken from the mean image data plane can be estimated to be as low as 1.564 nm and 1.239 nm, respectively.

The AlGaN MQWs can be easily identified by high-resolution transmission electron microscopy (HRTEM), as presented in Fig. 3(b). The alternately stacked bright and dark layers correspond to the AlN barriers and AlGaN QWs, respectively. The thicknesses of the AlN barriers and AlGaN QWs are 5.5 nm $\pm$ 0.1 nm and 2.5 $\pm$ 0.1 nm, which shows high consistence with the originally designed structure if taking the labeling errors during using length-marker of TEM into consideration. On the top of the AlN cladding layer, it can be observed a thin layer of oxidation with a thickness of 2.6 nm. Additionally, a linear scanning energy-dispersive X-ray spectroscopy analysis (EDXA) on the Al, Ga, and Si composition distribution is carried out across the microdisk cavities, as shown in Fig. 3(c). The atomic percentage for Al, Ga and Si compositions are not normalized here. Start from a depth around 18 nm, a periodical distribution of Ga composition across the MQWs area is clearly recognizable, which reaffirms the formation of AlGaN QWs with good uniformity of the Ga composition. Meanwhile, a clear cut-off in the Si and Al compositions is found at the depth around 150 nm, revealing that the AlN/Si interface is reached.

The photoluminescence (PL) measurements are conducted at the room-temperature (T$\sim$300 K) using a 193 nm ArF excimer pulsed laser as an excitation source. Excimer laser is operated with a pulse repetition rate of around 200 Hz and a pulse duration of $\sim$10 ns. The PL signals are probed by a multi-mode optical fiber coupled into the spectrometer (275 mm focus length, 10 μm slits, 1200 g/mm grating), which offers optical resolutions of 0.1 nm. The optical fiber head is fixed close to the AlGaN microdisks at an angle of $\sim$10° with the horizontal plane, facilitating the collection of optical leakage from the disk edge. Fig. 4 plots room-temperature PL spectra from AlGaN microdisk with increasing excitation energy densities. The spectra have been offset vertically for clarity. When the excitation densities are low, it can be clearly identified that the emission from AlGaN MQWs centers at 305.3 nm, with a bandwidth about 28.4 nm. As the pumping approaches the threshold energy density of 24.2 mJ/cm^2 (E_{th}), several spectral peaks emerge in the PL emission spectra, corresponding to the confined WGMs within the microdisk cavity, in which spectral peaks center at around wavelengths of $\sim$300 nm and $\sim$320 nm are labeled as Mode 1 and Mode 2, respectively. It is worth noting that this large lasing threshold is probably due to two reasons. First, the AlGaN MQWs grown on Si within the 150 nm-thick microdisk cavity may not be as efficient as the thick materials grown on sapphire or SiC substrates, which requires higher excitation densities to obtain enough optical gains and reach the threshold. Second, light source used in this study for pumping is with a wavelength of 193 nm, which will be absorbed by the AlN barriers as well. Concurrently,
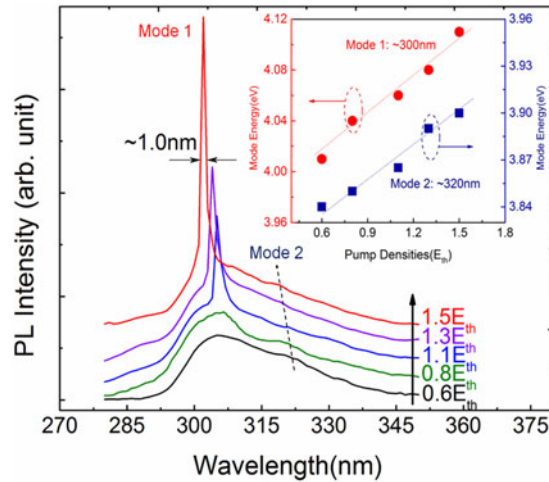
Fig. 4. Room-temperature PL spectra from an AlGaN/AlN microdisk with increasing the pumping energy densities. Inset shows the blueshift of the spectral WGM energies detected at around 300 nm and 320 nm. The PL spectra have been offset for clarity.

these modes are getting stronger with increasing the excitation powers due to the optical gains from amplified spontaneous emission. Above the E_{th}, the spectral peak at the center wavelength of ~300.1 nm become sharp and dominant throughout the PL spectra. Meanwhile, we can observe a continuous linear blueshift in the mode energies for both Mode 1 and 2 with increasing the excitation densities, as shown in the inset of Fig. 4. Specifically, the blueshift for Mode 1 and Mode 2 can be determined as ~100 meV and ~60 meV, respectively. In fact, as the excitation increases, photo-generated electrons and holes would occupy the band-edge energy states in the conduction or valence band. Attributed to the band-filling and charge screening effect, the bandgap of AlGaN QWs will become wider, leading to the blueshift in the emission spectra [28]. This is a common phenomenon with PL measurements for QW-based semiconductor structures. As the bandgap of AlGaN QWs becomes larger, its absorption coefficient under excitations will become smaller, resulting in a decrease of effective refractive index (n_{eff}) for wavelengths near or below the energy [29]. Therefore, the resonant modes need to shift to higher energy side to satisfy the standing-wave conditions, which leads to the blueshift in these spectral WGMs observed in Fig. 4:

$$m\lambda/n_{eff} = 2\pi r \tag{1}$$

where m presents the mode number in the azimuthal direction and r is the radius of the microdisk cavity).

Moreover, nonlinear increases in integrated PL intensities of the dominant WGM (Mode 1: ~300.1 nm) can be observed above the threshold, as plotted in Fig. 5. Such "s"-shape nonlinear increase entails typical characteristic of transition process from spontaneous emission to lasing emission. The upper and lower dotted lines are corresponding to the regions of spontaneous emission and stimulated emission, respectively. Taking the ratio of integrated PL intensities below and above the threshold extracted from this "s"-shape curve, the spontaneous emission coupling factor (β), defined as the fraction of spontaneous emission coupled into a cavity mode, can be roughly estimated to be 9.2×10^{-2} [30]. Here, we should point it out that the estimation of β using light output characteristic in a logarithmic scale is quite limited. More accurate fitting should be made to determine β by using rate equations [17], [18]. Fig. 5 also plots the linewidth evolution of the WGM at 300.1 nm as a function of pump densities. The spectral linewidth narrows from ~4.0 nm to ~1.0 nm as the excitation rises from 0.8 E_{th} to 1.3 E_{th}. A Q-factor of ~300 at the transparency can be roughly estimated using the relation $\lambda/\Delta\lambda$, where λ and $\Delta\lambda$ represent the wavelength and spectral linewidth, respectively. This value is relatively low perhaps due to the high dislocation density with the AlGaN MQWs grown on Si and increased intrinsic radiative losses with smaller disk radius [31].
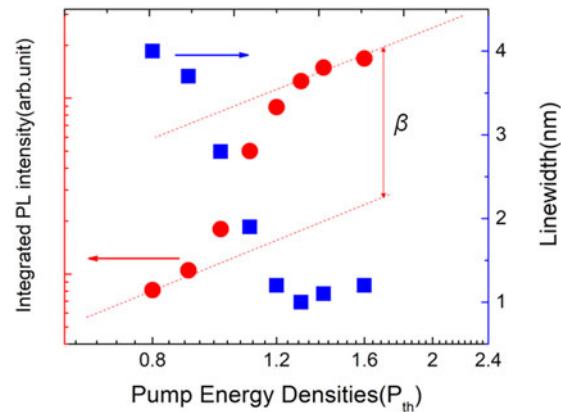
Fig. 5. Integrated PL intensities from an AlGaN/AlN microdisk and linewidth evolution under different pumping densities.

It may also be limited by the optical resolution of spectrometer used for measurements. Spectral narrowing is a clear sign of coherent light emission in the lasing regime, where the absorption has bleached as a result of positive feedback of gain mediums. It is worth noting, as the excitation is further increased to $1.6\,E_{th}$, the linewidth broadens to ~1.2 nm, which can be attributed to the free-carriers' absorption [17]. With an emission coupling factor $\beta \sim 9.2 \times 10^{-2}$, the Purcell factor ($F_p$) can be estimated to be ~0.1, where Purcell factor is defined by $F_p = \beta/(1 - \beta)$. Moreover, it can be also observed a sublinear increase in PL intensities as the pumping densities approach to the lasing threshold for the off-resonance wavelengths (~315 nm), which further confirms the onset of lasing within the microdisks.

Furthermore, 3D-FDTD simulations over a wavelength band from 280 nm to 350 nm have been conducted to identify the modal family. During the simulation, the dipoles are randomly placed in modeled microdisk cavity with the diameter of 1.0 μm, consistent with the size obtained from the SEM observation. Moreover, two plane monitors are placed at xy- and xz- plane to plot the $|E|^2$ distributions in the disk vertical and parallel directions. The n_{eff} of the AlGaN QWs is set to 2.33, which is lower than the GaN. Based on simulation results, the dominant lasing peak at ~301 nm can be attributed to first-order (n = 1) transverse-electric (TE) mode (m = 17) [32]. It should be noticed that this mode number is smaller from the calculation results from the standing-wave conditions (1) which uses the geometrical radius of the microdisk cavities. This is because the electromagnetic field of WGMs confined are actually located inner side of the disk boundary. The xy- and xz- plane electric-field energy intensity pattern of $TE_{1,17}$ around ~301.4 nm is plotted in Fig. 6(a) and (b), respectively. Regions shaded in red and blue represent the highest and lowest field intensities respectively, while the micro-disk boundary is defined by the red dashed line. The simulated resonances across the simulation range are shown in Fig. 6(c). The corresponding electric-field vector (***E***) patterns of $TE_{1,17}$ at ~301 nm and the radial $|E|^2$ distribution can be found in Fig. 6(b). Based on the 3D-FDTD simulation results, the optical confinement factor (Γ), defined as the overlap of the cavity mode with the active regions, is calculated to be ~0.21 (with 40 nm-thick active layers). Moreover, the mode spacings ($\Delta\lambda$) from the simulations with adjacent $TE_{1,18}$ and $TE_{1,16}$ are about ~13.9 nm and ~15.7 nm, respectively, which match well with spacings of ~14.2 nm and ~16.1 nm from the PL spectra (@1.5 E_{th}) as plotted in Fig. 6(c). And it is also consistent with the theoretical calculated mode spacings of 13.7 nm and 15.4 nm, which is roughly calculated by solving 2D Helmholtz equation via separation of variables [33], [34].

4. Conclusion

To conclude, we have demonstrated optically-pumped single-mode deep-ultraviolent lasing from 1-μm AlN microdisks with 5 pairs of AlGaN-based multiple quantum wells (MQWs) grown on Si
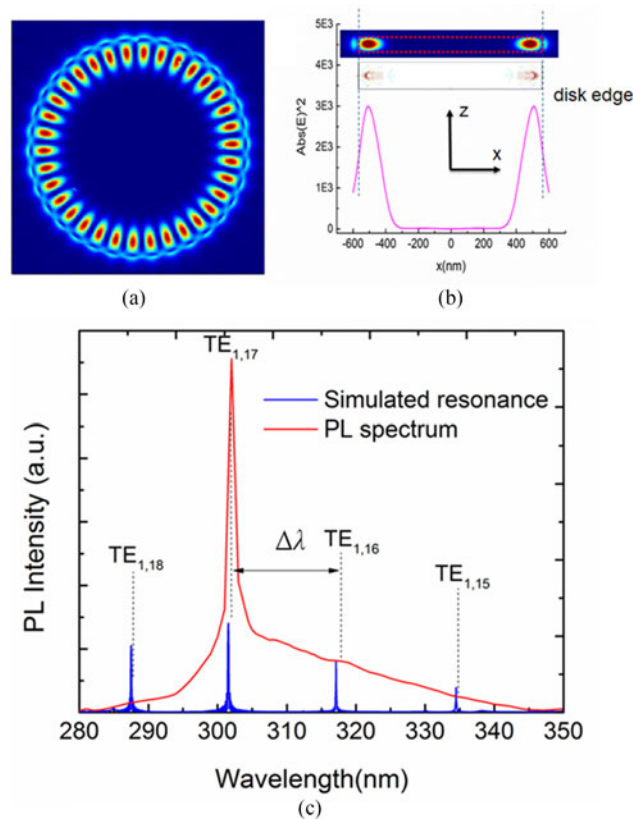
Fig. 6. Electric-field energy intensity patterns of whispering-gallery mode at ~301 nm (a) xy plane, (b) xz plane and (c) FDTD simulated resonances from a 1.0-μm microdisk.

(111) substrate at room temperature. The lasing wavelength centered at around 300.1 nm (UVB) with the linewidth of ~1.0 nm as the excitation exceeds the lasing threshold of ~24.2 mJ/cm^2. Three-dimensional FDTD simulations have verified that the spectral lasing mode belongs to the first-order transverse-electric (TE) whispering-gallery modes (WGMs) confined by the microdisk cavities. This work presents a significant step forwards to achieve single-mode operating microdisk lasers with low threshold on Si substrate, with emitting wavelengths reaching to the UVB range gained by the direct band emission from MOCVD-grown AlGaN MQWs. And it is also promising to serve as efficient deep UV coherent light sources for the photonic integration of the nitride-based semiconductor devices on the Si platform.

References

[1] H. Hirayama, N. Maeda, S. Fujikawa, S. Toyoda, and N. Kamata, "Recent progress and future prospects of AlGaN-based high-efficiency deep-ultraviolet light-emitting diodes," *Jpn. J. Appl. Phys.*, vol. 53, 2014, Art. no. 100209.

[2] M. Kneissl *et al.*, "Advances in group III-nitride-based deep UV light-emitting diode technology," *Semicond. Sci. Technol.*, vol. 26, 2011, Art. no. 014036.

[3] H. Yoshida, Y. Yamashita, M. Kuwabara, and H. Kan, "A 342-nm ultraviolet AlGaN multiple-quantum-well laser diode," *Nat. Photon.*, vol. 2, pp. 551–554, 2008.

[4] S. Gradečak, F. Qian, Y. Li, H.-G. Park, and C. M. Lieber, "GaN nanowire lasers with low lasing thresholds," *Appl. Phys. Lett.*, vol. 87, 2005, Art. no. 173111.

[5] S. Zhao, X. Liu, Y. Wu, and Z. Mi, "An electrically pumped 239 nm AlGaN nanowire laser operating at room temperature," *Appl. Phys. Lett.*, vol. 109, 2016, Art. no. 191106.

[6] L.-M. Chang *et al.*, "Laser emission from GaN photonic crystals," *Appl. Phys. Lett.*, vol. 89, 2006, Art. no. 071116.

[7] C.-F. Lai, "Lasing characteristics of a GaN photonic crystal nanocavity light source," *Appl. Phys. Lett.*, vol. 91, 2007, Art. no. 041101.

[8] R. Chen, H. D. Sun, T. Wang, K. N. Hui, and H. W. Choi, "Optically pumped ultraviolet lasing from nitride nanopillars at room temperature," *Appl. Phys. Lett.*, vol. 96, 2010, Art. no. 241101.

[9] A. C. Tamboli, E. D. Haberer, R. Sharma, K. H. Lee, S. Nakamura, and E. L. Hu, "Room-temperature continuous-wave lasing in GaN/InGaN microdisks," *Nat. Photon.*, vol. 1, pp. 61–64, 2007.

[10] D. Simeonov *et al.*, "High quality nitride based microdisks obtained via selective wet etching of AlInN sacrificial layers," *Appl. Phys. Lett.*, vol. 92, 2008, Art. no. 171102.

[11] I. Aharonovich *et al.*, "Low threshold, room-temperature microdisk lasers in the blue spectral range," *Appl. Phys. Lett.*, vol. 103, 2013, Art. no. 021112.

[12] Y. Zhang, X. Zhang, K. H. Li, Y. F. Cheung, C. Feng, and H. W. Choi, "Advances in III-nitride semiconductor microdisk lasers," *Phys. Status Solidi A.*, vol. 212, pp. 960–973, 2015.

[13] M. Athanasiou, R. Smith, B. Liu, and T. Wang, "Room temperature continuous–wave green lasing from an InGaN microdisk on silicon," *Sci. Rep.*, vol. 4, 2014, Art. no. 7250.

[14] Y. Zhang, Z. Ma, X. Zhang, T. Wang, and H. W. Choi, "Optically pumped whispering-gallery mode lasing from 2-μm GaN micro-disks pivoted on Si," *Appl. Phys. Lett.*, vol. 104, 2014, Art. no. 221106.

[15] H. W. Choi *et al.*, "Lasing in GaN microdisks pivoted on Si," *Appl. Phys. Lett.*, vol. 89, 2006, Art. no. 211101.

[16] M. Mexis *et al.*, "High quality factor nitride-based optical cavities: Microdisks with embedded GaN/Al(Ga)N quantum dots," *Opt. Lett.*, vol. 36, no. 12, 2011, Art. no. 2203.

[17] M. Bürger *et al.*, "Lasing properties of non-polar GaN quantum dots in cubic aluminum nitride microdisk cavities," *Appl. Phys. Lett.* vol. 103, 2013, Art. no. 021107.

[18] J. Sellés *et al.*, "Deep-UV nitride-on-silicon microdisk lasers," *Sci. Rep.*, vol. 6, 2016, Art. no. 21650.

[19] J. Sellés *et al.*, "III-Nitride-on-silicon microdisk lasers from the blue to the deep ultra-violet," *Appl. Phys. Lett.*, vol. 109, 2016, Art. no. 231101.

[20] K. Kamiya, Y. Ebihara, K. Shiraishi, and M. Kasu, "Structural design of AlN/GaN superlattices for deep-ultraviolet light-emitting diodes with high emission efficiency," *Appl. Phys. Lett.*, vol. 99, 2011, Art. no. 151108.

[21] D. Bayerl, S. M. Islam, C. M. Jones, V. Protasenko, D. Jena, and E. Kioupakis, "Deep ultraviolet emission from ultra-thin GaN/AlN heterostructures," *Appl. Phys. Lett.*, vol. 109, 2016, Art. no. 241102.

[22] T. Takano, Y. Narita, A. Horiuchi, and H. Kawanishi, "Room-temperature deep-ultraviolet lasing at 241.5 nm of AlGaN multiple-quantum-well laser," *Appl. Phys. Lett.*, vol. 84, 2004, Art. no. 3567.

[23] Z. Lochner *et al.*, "Deep-ultraviolet lasing at 243 nm from photo-pumped AlGaN/AlN heterostructure on AlN substrate," *Appl. Phys. Lett.*, vol. 102, 2013, Art. no. 101110.

[24] X.-H. Li *et al.*, "Low-threshold stimulated emission at 249 nm and 256 nm from AlGaN-based multiple-quantum-well lasers grown on sapphire substrates," *Appl. Phys. Lett.*, vol. 105, 2014, Art. no. 141106.

[25] Y. Tian *et al.*, "Stimulated emission at 288 nm from silicon-doped AlGaN-based multiple-quantum-well laser," *Opt. Exp.*, vol. 23, pp. 11334–11340, 2015.

[26] J. Yan, Y. Tian, X. Chen, Y. Zhang, J. Wang, and Ji. Li, "Deep ultraviolet lasing from AlGaN multiple-quantum-well structures," *Phys. Status Solidi C*, vol. 13, pp. 228–231 2016.

[27] J.-M. Lee, K.-M. Chang, I.-H. Lee, and S.-J. Park, "Cl$_2$-based dry etching of GaN and InGaN using inductively coupled plasma the effects of gas additives," *J. Electrochem. Soc.*, vol. 147, no. 5, pp. 1859–1863, 2000.

[28] L.-H. Peng, C.-W. Chuang, and L.-H. Lou, "Piezoelectric effects in the optical properties of strained InGaN quantum wells," *Appl. Phys. Lett.*, vol. 74, 1999, Art. no. 795.

[29] B. R. Bennett, R. A. Soref, and J. A. Del Alamo, "Carrier-induced change in refractive index of InP, GaAs and InGaAsP," *IEEE J. Quantum Electron.*, vol. 26, no. 1, pp. 113–122, Feb. 1990.

[30] H. Takashima, H. Fujiwara, S. Takeuchi, K. Sasaki, and M. Takahashi, "Control of spontaneous emission coupling factor β in fiber-coupled microsphere resonators," *Appl. Phys. Lett.*, vol. 92, 2008, Art. no. 071115.

[31] C. X. Ren, T. J. Puchtler, T. Zhu, J. T. Griffiths, and R. A. Oliver, "Defects in III-nitride microdisk cavities," *Semicond. Sci. Technol.*, vol. 32, 2017, Art. no. 033002.

[32] W. W. Chow and M. Kneissl, "Laser gain properties of AlGaN quantum wells," *J. Appl. Phys.*, vol. 98, 2005, Art. no. 114502.

[33] M. Kneissl, M. Teepe, N. Miyashita, N. M. Johnson, G. D. Chern, and R. K. Chang, "Continuous wave operation of a spiral-shaped microcavity laser," *Appl. Phys. Lett.*, vol. 84, 2004, Art. no. 2485.

[34] Y. Zhang, C. Feng, T. Wang, and H. W. Choi, "GaN hemispherical micro-cavities," *Appl. Phys. Lett.*, vol. 108, 2016, Art. no. 031110.